The Functional Rotational Workspace of a Human-Robot System can be Influenced by Adjusting the Telemanipulator Handle Orientation

Esther I. Zoller, *Student Member, IEEE*, Nicolas Gerig, Philippe C. Cattin, *Member, IEEE*, and Georg Rauter, *Member, IEEE*

***Abstract*—The handle design of telemanipulation master devices has not been extensively studied so far. However, the master device handle is an integral part of the robotic system through which the user interacts with the system. Previous work showed that the size and shape of the functional rotational workspace of the human-robot system and its usability are influenced by the design of the master device handle. Still, in certain situations, e.g., due to user preference, a specific grasp type handle might be desired. Therefore, in this article, we provide a systematic approach on how to assess and adjust the functional rotational workspace of a human-robot system. We investigated the functional rotational workspace with two exemplary grasp type handles and two different mounting orientations for each handle. The results showed that by adapting the handle orientation in the home configuration of the telemanipulator, the functional rotational workspace of the human-robot system can be adjusted systematically to cover more of the mechanical workspace of the master device. Finally, we deduct recommendations on how to choose and adjust a telemanipulator handle.**

***Index Terms*—Human-robot interaction, telemanipulation, human factors and ergonomics.**

I. Introduction

Teleoperated surgical robots are becoming more and more popular. In 2018, an estimate of more than one million robotic surgeries had been performed worldwide with da Vinci systems alone [1]. In these surgeries, the surgeon controls the surgical instrument (slave) via a remote input device (master). The spatial separation of the surgeon and the instrument allows the master device motions to be processed before they are transferred to the slave. The master device motions can, for example, be downscaled, thus allowing more precise instrument motions than a human could perform [2]. Or, if the master moves into a previously defined forbidden region, the master device motions can be completely ignored, thereby preventing the slave from damaging delicate tissue [3].

However, the use of such robotic systems also bears many challenges. Most of these systems do not provide haptic feedback to the user [4], [5], meaning that the surgeons have to rely solely on visual information. Also, the mechanical workspace of the master device is limited and therefore often does not allow all motions the user would like to perform. This is commonly addressed by indexing, which allows the operator to decouple the master device motion from the slave and reposition the master device end-effector within its workspace [6]–[8]. While indexing disrupts the workflow of the operator and can become cumbersome [9], it has also been described to be very useful for surgical teleoperation [7]. Other methods to overcome the limited workspace of the master device include scaling control, ballistic control, rate control, drift control, or a combination thereof [10]. However, when applied to rotational degrees of freedom (DoF) of the master device, all of these methods lead to a variable misalignment between the master and slave orientations. Such variable master-slave misalignment makes it difficult for the operator to understand how master rotations map to slave rotations [7]. Kim *et al.* [11] showed that task performance decreases with increasing orientational master-slave misalignment. It can be assumed that in addition to decreasing performance, variable master-slave misalignment also increases the cognitive workload of the operator, as they permanently have to adapt to the changing master-slave misalignment. Thus, the importance of a master device that allows the operator to perform the necessary orientational motions without indexing seems evident, especially as Boessenkool *et al.* [12] found that in teleoperated fine positioning tasks, the control of the tool orientation is particularly difficult, even without master-slave misalignment.

A lot of effort has been invested in the development of high-fidelity haptic master devices with a large rotational workspace. The results include devices such as the Virtuose 6D Desktop (Haption S.A., Soulgé-sur-Ouette, France) [13], the Phantom Premium (3D Systems, Rock Hill, USA) [14], or the sigma.7 (Force Dimension, Nyon, Switzerland) [15]. However, in a teleoperation setting, the human operator interacts with

Manuscript received December 1, 2019; revised June 17, 2020 and August 4, 2020; accepted August 24, 2020. Date of publication September 28, 2020; date of current version June 16, 2021. This work was supported by the Werner Siemens Foundation through the MIRACLE project. This article was recommended for publication by Associate Editor Dr. Christian Duriez and Editor-in-Chief L. Jones upon evaluation of the reviewers' comments. *(Corresponding author: Esther I. Zoller.)*

Esther I. Zoller, Nicolas Gerig, and Georg Rauter are with the BIROMED-Lab, Department of Biomedical Engineering, University of Basel, 4123 Allschwil, Switzerland (e-mail: esther.zoller@unibas.ch; nicolas.gerig@unibas.ch; georg.rauter@unibas.ch).

Philippe C. Cattin is with the CIAN, Department of Biomedical Engineering, University of Basel, 4123 Allschwil, Switzerland (e-mail: philippe.cattin@unibas.ch).

This article has supplementary downloadable material available at https://ieeexplore.ieee.org, provided by the authors.

Digital Object Identifier 10.1109/TOH.2020.3027261

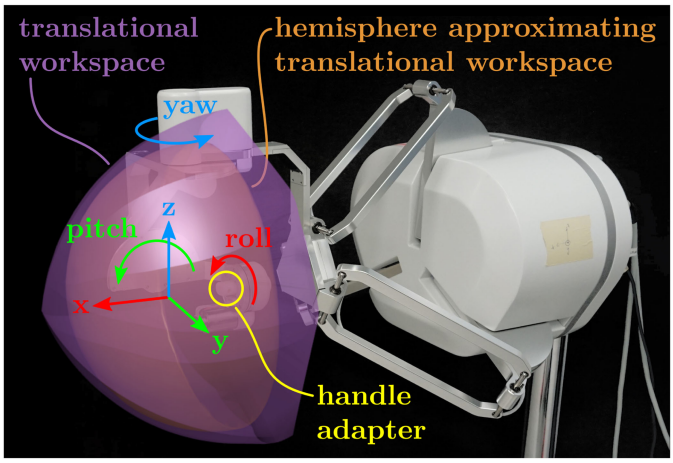

Fig. 1. The lambda.6 haptic device. The delta structure is used to position the end-effector, while the serial structure is responsible for the orientation of the end-effector. Different handles can be mounted to the handle adapter. The experimentally determined translational workspace (purple) encloses a hemisphere (orange) with a radius of 150 mm.

the master device, and therefore its end-effector motion is not only constrained by the device mechanics, but also by the functional anatomy of the operator's hand and wrist [16]. The design of the master device handle influences the hand and finger position during operation [17], which in turn influences the motion capability of the wrist [18]. These anatomical constraints could explain why surgeons do not rest their forearms on the provided armrest during robot-assisted surgery about one third of the time [19]. Instead, they lift their forearms to maneuver the master device end-effector to poses otherwise not reachable. However, due to ergonomic reasons, operators of robot-assisted surgical systems should maintain their forearms resting comfortably on the provided armrest in a neutral position [20], [21]. Taking this ergonomic recommendation into account, we define the functional rotational workspace of the human-robot system as the intersection of the mechanical rotational workspace of the master device and the anatomical rotational workspace of the operator's hand and wrist with a given grasp type and a weight-supported arm posture. We believe that such a task-independent handle property allows a more informed choice of handle candidates for both multi-task and task-specific teleoperation settings. For the scope of this work, we consider the functional rotational workspace of the human-robot system with one specific weight-supported arm posture, namely with the forearm strapped to an armrest in a horizontal posture.

In a previous study, we assessed the functional rotational workspace of nine different grasp type handles and showed that it is critically influenced by the design of the master device handle [22]. While the results indicated that for certain grasp type handles, the mechanical rotational workspace of the master device and the anatomical rotational workspace of the operator's hand and wrist were not concentric, they did not reveal to what extent this was due to the grasp type or the home wrist configuration. Thus, for these grasp type handles, the functional rotational workspace of the human-robot system could potentially be increased by improving the alignment of the mechanical rotational workspace of the master device with the anatomical rotational workspace of the operator's hand and wrist. Improved workspace alignment could be achieved by either adjusting the mounting orientation of the grasp type handles or by rotating the whole master device.

TABLE I
JOINT LIMITS OF THE LAMBDA.6 DEVICE AND LOCATION OF SOFTWARE FEATURES TO PROTECT THE DEVICE

Joint	Mechanical limits	Virtual walls	Visual warnings
Delta joints	$-55°$ / $+89°$	$-45°$ / $+80°$	$-52.5°$ / $+87.5°$
Yaw (ψ)	$-83°$ / $+79°$	$\pm 75°$	$\pm 77.5°$
Pitch (θ)	$-69°$ / $+72°$	$\pm 65°$	$\pm 67.5°$
Roll (φ)	$-144°$ / $+150°$	$\pm 140°$	$\pm 142.5°$

To verify this hypothesis, we investigate whether systematically adjusting the mounting orientation of specific grasp type handles allows increasing the functional rotational workspace of the human-robot system. The investigations were carried out on two exemplary grasp type handles for two different mounting orientations. In addition, we explore the usability of the different grasp type handles to assess if an adjustment of the handle mounting orientation also affects the handle usability.

In Section II, the experimental setup is described. Section III presents a summary of the previously published functional rotational workspace assessment study. The functional rotational workspace adjustment study is described in detail in Section IV, followed by a discussion in Section V and conclusions in Section VI.

II. EXPERIMENTAL SETUP

A. Haptic Input Device

We used a customized, handleless, six DoF lambda.6 haptic device (Force Dimension, Nyon, Switzerland), which was designed for use with the right hand (see Fig. 1). At the end-effector of the lambda.6 device, an adapter allows for easy mounting of different handles. The device's translational workspace has been determined experimentally and encloses a hemisphere with a radius of 150 mm (see Fig. 1). The experimentally determined joint limits of the haptic device are provided in Table I.

B. Functional Rotational Workspace Evaluation System

To assess the functional rotational workspace of the human-robot system with each handle, we built a custom application using CHAI3D [23] and the Force Dimension SDK (version 3.7.3.3210). The application's core was a virtual environment with a static hemisphere and a capsule whose position was fixed at the center of the hemisphere (see Fig. 2). A black line exiting from the capsule's tip was used as a laser pointer, indicating where the capsule's longitudinal axis collided with the hemisphere surface. The capsule's orientation was controlled by the orientation of the lambda.6 end-effector through a direct mapping. To protect the device from any damage by the user, virtual walls were implemented before reaching the mechanical joint limits of the device. In addition, visual

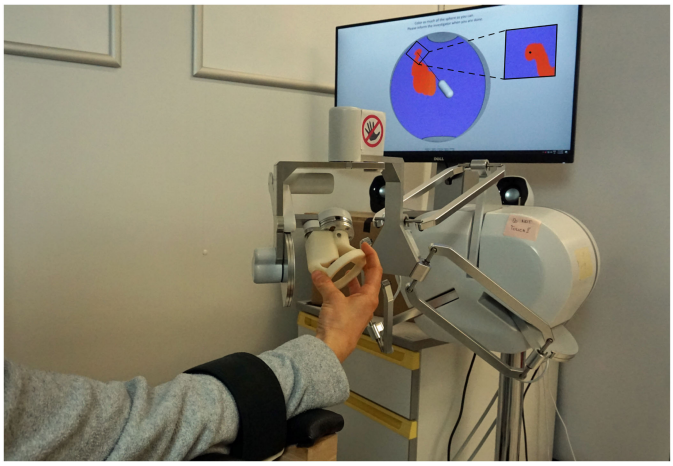

Fig. 2. System setup: The participant is seated in front of the lambda.6 haptic device with the right forearm strapped to the armrest, thus fixing the wrist position relative to the device. The extreme wrist orientation (high pitch and yaw angles of the end-effector) was chosen for visualization purposes such that the grasp type is clearly visible. The virtual environment is displayed on a screen placed behind the lambda.6. The violet area of the hemisphere marks the pitch/yaw workspace of the lambda.6 that the participant is trying to color. The square at the top right shows a close-up of the area the end-effector is currently pointing at.

warnings were added to the virtual environment to let the user know that the device end-effector is approaching the mechanical workspace boundaries. The location of the virtual walls and visual warnings is provided in Table I. The virtual walls were constructed as spring/damper systems whose characteristics are displayed in Table II. The border of the mechanical pitch/yaw workspace, i.e., where the virtual walls were placed, was visualized with a black line on the inner surface of the hemisphere. The mechanical pitch/yaw workspace was colored violet and the area outside the border grey. To interact with the virtual environment, the user was seated in front of the lambda.6 in a seating posture of their own choice. The right forearm of the user was aligned with the roll axis of the device in its home configuration to achieve optimal wrist dexterity. The forearm of the user was strapped to the armrest such that the wrist position relative to the device was fixed. This was necessary to create controlled experimental conditions, but it also ensured an ergonomic, weight-supported forearm posture. The pro-/supination of the forearm was not restricted (see Fig. 2).

Upon the start of the application, the lambda.6 was gravity compensated, and the user was asked to move the device handle (and thus the capsule in the virtual environment) to a neutral, i.e., 0°, pitch and yaw orientation. Once this orientation was reached, the functional pitch/yaw assessment started. The inner surface of the hemisphere was colored wherever the laser pointer collided with it (see Fig. 2). Using only the motion allowed by the hand and wrist, the user tried to color as much of the virtual hemisphere as possible, thereby exploring the pitch/yaw workspace of the lambda.6. During this phase, the application recorded in the background which of nine discrete pitch/yaw configurations spread on the hemisphere surface were reached. These discrete pitch/yaw configurations were at 5° from the virtual walls as well as at the neutral angle (0°) on both the pitch and yaw axes, resulting in a total of nine

TABLE II
CHARACTERISTICS OF THE VIRTUAL WALLS IMPLEMENTED BEFORE THE DEVICE JOINT LIMITS

	Delta joints	Yaw	Pitch	Roll
Stiffness [Nm/rad]	6.0	4.0	4.0	3.0
Damping [Nm/(rad/s)]	0.06	0.04	0.04	0.03

roll assessment points $P_{\theta\psi}$. Whenever the user decided that they could not reach any further pitch/yaw configurations, the application could be switched to the functional roll workspace assessment by the experimenter using a foot pedal.

A new scene appeared on the screen where a study-dependent selection of the nine discrete pitch/yaw configurations was shown on the hemisphere surface. These pitch/yaw configurations were used for the assessment of the functional roll workspace. The user was asked to move to one of these pitch/yaw configurations. Once there, the lambda.6 held its end-effector at the respective pitch/yaw configuration using a spring/damper system with the same characteristics as the virtual walls at the boundaries of the pitch and yaw workspace (see Table II). The rotation around the roll axis of the device and all translational DoF were free. The user was asked to explore the roll range that they could reach at the respective pitch/yaw configuration by rotating the handle around the axis of the last serial link of the device. The color of the roll assessment point changed with the range of reached roll angles. Whenever the user decided that they could not reach any additional roll angles at the given pitch/yaw configuration, the application could be switched to the next pitch/yaw configuration by the experimenter using a foot pedal.

During both the pitch/yaw and roll workspace assessments, the application recorded the following device data: end-effector position, end-effector rotation, and the forces and torques applied by the device on the end-effector. In addition, at the end of both the pitch/yaw and roll workspace assessments, the texture map of the virtual hemisphere was saved.

III. FUNCTIONAL ROTATIONAL WORKSPACE ASSESSMENT STUDY

This section consists of a summary of a previously published study [22], where we evaluated the functional rotational workspace of a human-robot system with the forearm strapped to an armrest in a horizontal posture for different grasp type handles. It presents the basis for the functional rotational workspace adjustment study presented in Section IV.

A. Summary of Design and Procedure

The functional rotational workspace for the lambda.6 was assessed with the following nine different grasp type handles: *power disk*, *quadpod*, *power sphere*, *tripod*, *precision disk*, *parallel extension*, *fixed hook*, *writing tripod*, and *adducted thumb*. These handles cover a selection of the 33 grasp types described in [24], which we considered being appropriate for six DoF telemanipulation tasks with the lambda.6 haptic device [25]. Each of the nine participants performed the

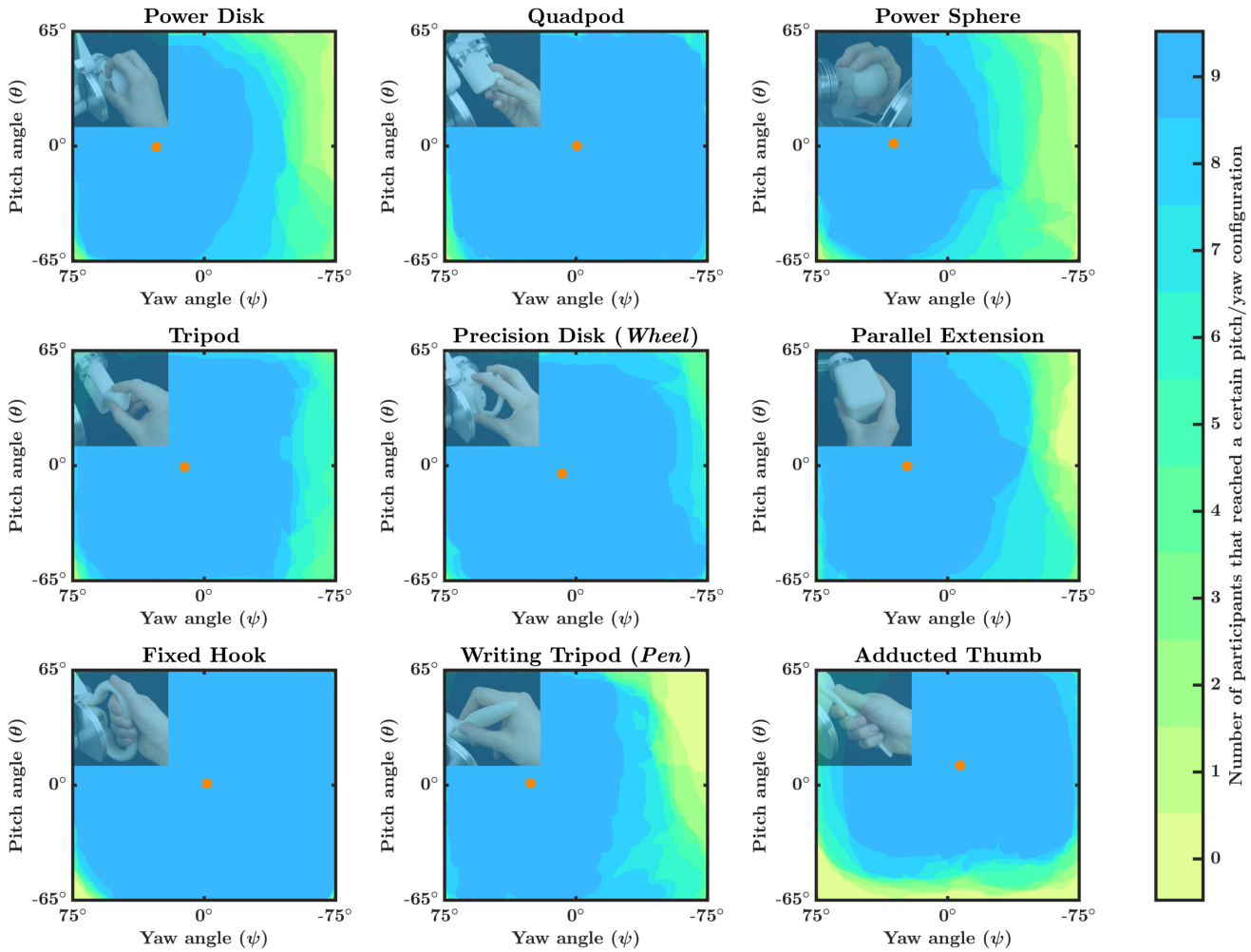

Fig. 3. Functional pitch/yaw workspace (within the virtual wall limits set to protect the device) of the nine participants with a fixed horizontal forearm posture for each of the nine grasp type handles. The workspace color indicates the number of participants that reached a certain pitch/yaw configuration. In addition, the center of mass of the functional pitch/yaw workspace that was reached by all nine participants, $C_{\theta/\psi}$, is indicated by the orange circles. The overlayed pictures depict the investigated handles and the corresponding grasp type.

functional rotational workspace assessment experiments with all nine handles using the application described in Section II-B, with their forearm strapped to the armrest in a horizontal posture. For the roll workspace assessment, only the points $P_{\theta\psi}$ at pitch/yaw configurations that the participant reached during the coloring phase were displayed.

B. Summary of Results

The pitch/yaw workspace that was reached by all participants with a fixed horizontal forearm posture was dependent on the grasp type handle (see Fig. 3). While the pitch/yaw workspace reached by all participants covered more than 90% of the mechanical pitch/yaw workspace of the lambda.6 with certain handles (e.g., the fixed hook and quadpod grasp handles), it covered only about half of the mechanical pitch/yaw workspace of the lambda.6 with other handles (e.g., the power disk and power sphere grasp handles).

The roll workspace that was reached by all participants with a fixed horizontal forearm posture was also dependent on the grasp type handle (see Fig. 4). For some handles, such as the fixed hook and adducted thumb grasp handles, the roll workspace reached by all participants was relatively symmetric around $0°$ roll, while for others, such as the precision disk grasp handle, it was completely in the negative range of the mechanical roll workspace for several roll assessment points.

IV. Functional Rotational Workspace Adjustment Study

A. Rationale

In the pre-study described in Section III, some of the tested handles showed a functional rotational workspace with a fixed horizontal forearm posture that was clearly off-centered in the mechanical rotational workspace of the haptic device (see Fig. 3). For example, the *power disk*, *power sphere*, *tripod*, *parallel extension*, and *writing tripod* grasp handles all showed a functional pitch/yaw workspace extending to the mechanical workspace boundary in the positive yaw direction,

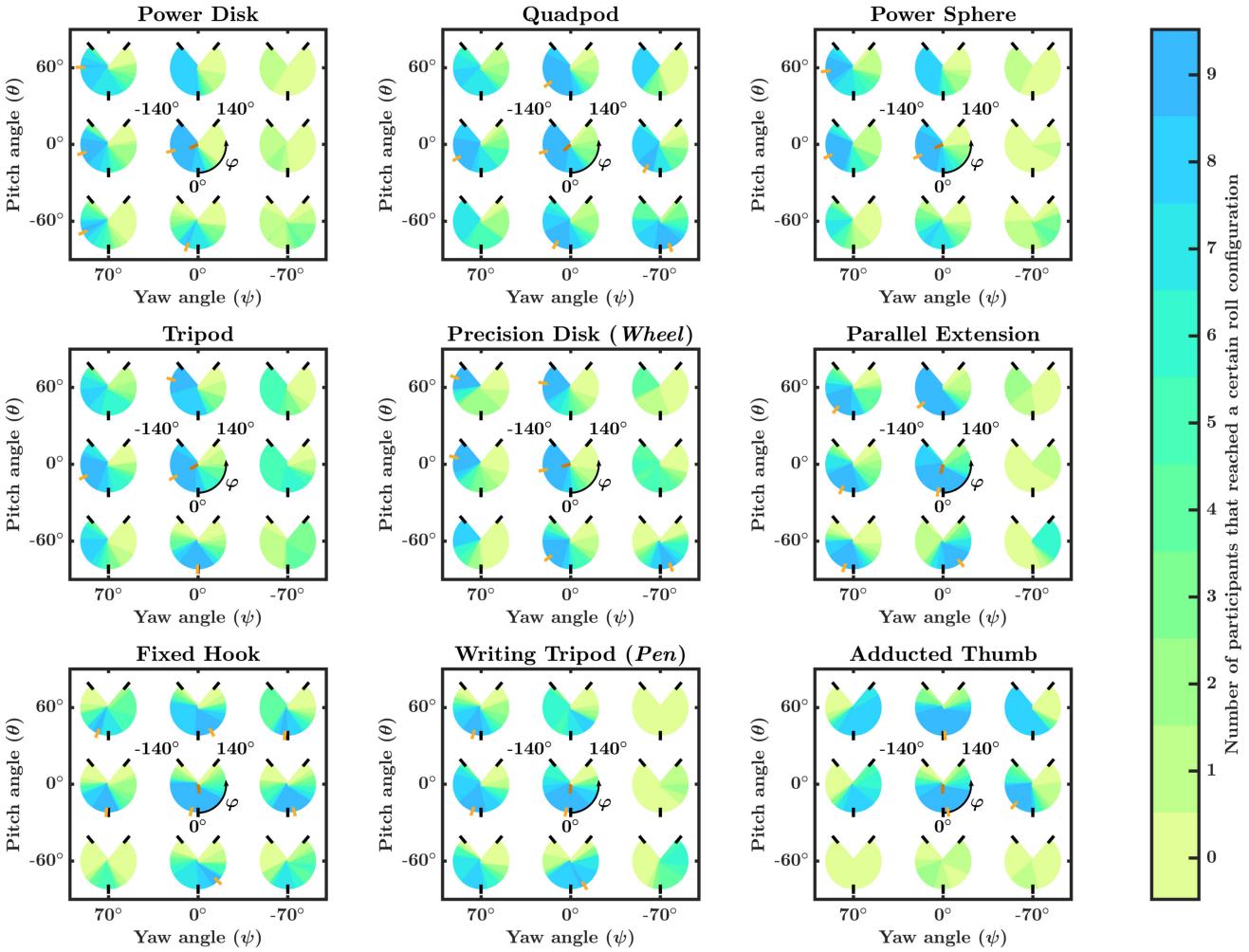

Fig. 4. Functional roll workspace of the nine participants with a fixed horizontal forearm posture at all nine discrete roll assessment points $P_{\theta\psi}$ spread in the pitch/yaw workspace for each of the nine grasp type handles. The colored circle sectors depict the device roll workspace ranging from $-140°$ to $140°$. At these limits, the virtual walls for the roll axis were placed. The color indicates the number of participants that reached a certain roll configuration. In addition, the center of the functional roll workspace that was reached by all nine participants, $C_{\varphi,P_{\theta\psi}}$, is visualized by the light orange ticks for each of the nine roll assessment points. No light orange tick means that no roll configuration was reached by all participants. The dark orange tick at the center of the central circle sector depicts the weighted average center of the functional roll workspace that was reached by all nine participants, $\overline{C}_{\varphi}$.

while the mechanical workspace boundary in the negative yaw direction was hardly reached.

Furthermore, the *power disk*, *quadpod*, *power sphere*, *tripod*, *precision disk*, and *parallel extension* grasp handles showed a functional roll workspace extending to the mechanical workspace boundary in the negative roll direction for some roll assessment points, while the mechanical workspace boundary in the positive roll direction was hardly reached (see Fig. 4).

These results suggest that the overlap of the anatomical workspace of the human hand/wrist and the mechanical workspace of the lambda.6 was not optimal for the above-mentioned handles. However, surgeons prefer working with instrument handles they are most familiar with [26], which might well be handles that did not show a large or centered functional rotational workspace with a fixed horizontal forearm posture. Therefore, we conducted a second study where we investigated whether we can systematically adjust the overlap of the anatomical workspace of the human hand/wrist and the mechanical workspace of the lambda.6 for two exemplary grasp type handles. The following hypotheses were to be tested:

- H1: Systematically adjusting the pitch/yaw mounting orientation of a grasp type handle with an off-center functional pitch/yaw workspace increases the functional pitch/yaw workspace of that handle.
- H2: Systematically adjusting the roll mounting orientation of a grasp type handle with an off-center functional roll workspace increases the functional roll workspace of that handle.

Additionally, we investigated whether an adjustment of the pitch/yaw mounting orientation of a handle led to a change in the functional roll workspace of that handle and vice versa. Whether the performed adjustments led to a change in the computed pitch/yaw and roll workspace center offsets was analyzed as well. Last but not least, we also assessed whether an adjustment of the mounting orientation of a handle led to a difference in the usability of that handle.

TABLE III
FUNCTIONAL WORKSPACE CENTER OFFSET FROM THE CENTER OF THE MECHANICAL WORKSPACE OF THE LAMBDA.6 FOR ALL NINE GRASP TYPE HANDLES IN BOTH THE PITCH/YAW ($C_{\theta/\psi}$) AND ROLL ($\overline{C}_{\varphi}$) SPACE AS WELL AS THE WEIGHTED AVERAGE ROLL WORKSPACE RANGE THAT WAS REACHED BY ALL PARTICIPANTS ($\overline{R}_{\varphi}$)

Handle	$C_{\theta/\psi}$ [°]	$\|C_{\theta/\psi}\|$ [°]	$\overline{C}_{\varphi}$ [°]	$\overline{R}_{\varphi}$ [°]
Power Disk	(-0.5, 27.2)	27.2	-65.2	40.4
Quadpod	(0.1, -0.6)	0.6	-48.6	75.3
Power Sphere	(1.4, 30.8)	30.8	-67.3	41.5
Tripod	(-0.8, 11.1)	11.2	-58.8	56.8
Precision Disk	(-4.5, 7.9)	9.1	-76.3	64.7
Parallel Extension	(-0.3, 23.0)	23.0	-14.7	84.0
Fixed Hook	(0.9, -1.7)	1.9	5.6	68.2
Writing Tripod	(1.1, 25.8)	25.8	-3.7	39.6
Adducted Thumb	(11.2, -7.2)	13.3	-4.4	64.6

B. Design & Procedure

The exemplary grasp type handles for this study were chosen based on the results from the pre-study. We wanted to select handles that already performed well but had a considerable offset for the center of the functional rotational workspace with a fixed horizontal forearm posture compared to the center of the rotational workspace of the device. Such an offset indicates a potential for further improvement of the functional rotational workspace size.

To investigate whether we could systematically adjust the functional pitch/yaw workspace to be larger and more centered in the mechanical pitch/yaw workspace of the lambda.6, we had to select an exemplary grasp type handle where the functional pitch/yaw workspace was not centered in the mechanical pitch/yaw workspace of the lambda.6. Therefore, we calculated the center of mass of the functional pitch/yaw workspace, $C_{\theta/\psi}$, on the recorded texture maps of the pre-study for all grasp type handles (see Fig. 3). The three handles with the highest pitch/yaw workspace center offset were the *power sphere*, the *power disk*, and the *writing tripod* grasp handles (see Table III). We chose the *writing tripod* grasp handle (*Pen*) because the *writing tripod* grasp handle showed a higher mean usability score than the other two handles (60.22 / 100 for the *writing tripod* grasp handle versus 49.43 / 100 and 39.13 / 100 for the *power disk* and *power sphere* grasp handles) [22].

From the data of the pre-study, we calculated the roll range reached by all participants, $R_{\varphi,P_{\theta\psi}}$, for each roll assessment point $P_{\theta\psi}$. Subsequently, we calculated how much the center of $R_{\varphi,P_{\theta\psi}}$, $C_{\varphi,P_{\theta\psi}}$, deviated from 0° roll. This was done for each roll assessment point $P_{\theta\psi}$ and each grasp type handle (see Fig. 4). We consider a roll workspace that is symmetric around 0° more important in the center of the pitch/yaw workspace than at its borders. Thus, we computed the weighted average roll workspace center that was reached by all participants, $\overline{C}_{\varphi}$, using a discrete approximation of a 3 x 3 Gaussian blur kernel (see Fig. 4):

$$\overline{C}_{\varphi} = \frac{\sum_{\theta}\sum_{\psi}\left(w_{\theta\psi}C_{\varphi,P_{\theta\psi}}\right)}{c_{\overline{C}_{\varphi}}}, \tag{1}$$

where $w_{\theta\psi}$ are the weights of the Gaussian blur kernel:

$$w_{\theta\psi} = \begin{bmatrix} 1 & 2 & 1 \\ 2 & 4 & 2 \\ 1 & 2 & 1 \end{bmatrix}, \tag{2}$$

$C_{\varphi,P_{\theta\psi}}$ are the centers of the roll range reached by all participants for each roll assessment point $P_{\theta\psi}$, and $c_{\overline{C}_{\varphi}}$ is the normalizing factor:

$$c_{\overline{C}_{\varphi}} = \sum_{\theta}\sum_{\psi} w_{\theta\psi}\,, \forall\ \theta,\ \psi \text{ where } R_{\varphi,P_{\theta\psi}} > 0. \tag{3}$$

The three handles with the highest offset of the weighted average workspace center $\overline{C}_{\varphi}$ were the *power disk*, the *power sphere*, and the *precision disk* grasp handles (see Table III). To choose one of these handles for this study, we also computed the weighted average roll workspace range that was reached by all participants, $\overline{R}_{\varphi}$. Again, we used a discrete approximation of a 3 x 3 Gaussian blur kernel for the weighting of the different roll assessment points:

$$\overline{R}_{\varphi} = \frac{\sum_{\theta}\sum_{\psi}\left(w_{\theta\psi}R_{\varphi,P_{\theta\psi}}\right)}{c_{\overline{R}_{\varphi}}}, \tag{4}$$

where $w_{\theta\psi}$ are the weights of the Gaussian blur kernel (see Eq. 2), $R_{\varphi,P_{\theta\psi}}$ are the roll ranges reached by all participants for each roll assessment point $P_{\theta\psi}$, and $c_{\overline{R}_{\varphi}}$ is a normalizing factor:

$$c_{\overline{R}_{\varphi}} = \sum_{\theta}\sum_{\psi} w_{\theta\psi}. \tag{5}$$

We chose the *precision disk* grasp handle (*Wheel*) to investigate whether we could systematically adjust the functional roll workspace to be larger and more centered in the mechanical roll workspace of the lambda.6, because $\overline{R}_{\varphi}$ was considerably higher for the *precision disk* grasp handle than for the *power disk* and *power sphere* grasp handles (see Table III).

To investigate whether a systematic adjustment of the overlap between the anatomical workspace of the human hand/wrist and the mechanical workspace of the lambda.6 is possible for the two selected grasp type handles, we designed a *pitch/yaw adjusted writing tripod* grasp handle (*AdjPen*) and a *roll adjusted precision disk* grasp handle (*AdjWheel*). For the *AdjPen* we took the same handle shape as for the *Pen* but attached it to the mounting adapter of the lambda.6 with a pitch and yaw rotation of 1.1° and 25.8°, respectively (see Fig. 5). Analogously, the *AdjWheel* was created using the same handle shape as for the *Wheel*, but attaching it to the mounting adapter for the lambda.6 with a roll rotation of -76.3° (see Fig. 5). These rotations correspond to the computed workspace center offsets of the *Pen* and *Wheel*.

Thus, the handles of interest for this study were the *Pen*, the *AdjPen*, the *Wheel*, and the *AdjWheel* (see Fig. 5). The study had a cross-over (within-subjects) design with the handle as the only independent variable.

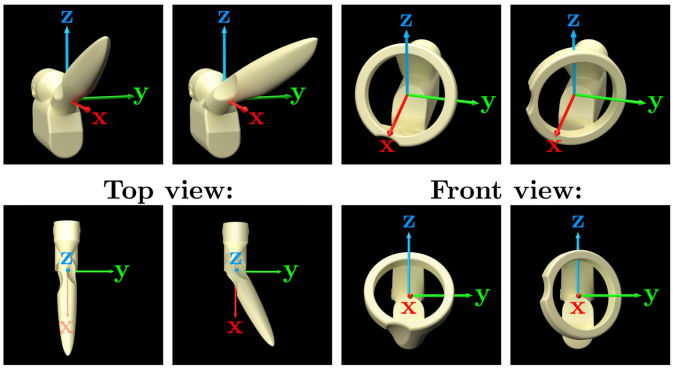

Fig. 5. The four handles investigated in the functional rotational workspace adjustment study (left to right): *original writing tripod* grasp handle (*Pen*), *pitch/yaw adjusted writing tripod* grasp handle (*AdjPen*), *original precision disk* grasp handle (*Wheel*), and *roll adjusted precision disk* grasp handle (*AdjWheel*).

C. Protocol

Before starting the functional rotational workspace assessment with any given handle, the participant was shown an instructional video that explained how the handle should be grasped for the following trial. The functional rotational workspace of the human-robot system was then assessed with the different handles using the workspace evaluation system described in Section II-B. Only the right hand of the participant was examined as both the device and the handles were designed for use with the right hand. The forearm of the participant was strapped to the armrest to achieve controlled experimental conditions. The experimenter continuously observed the grasp type of the participant and instructed the participant to restore the instructed grasp type when necessary. At the end of the experiments with any given handle, the participant was asked to fill out a custom questionnaire (see supplemental material).

For the roll workspace assessment, all nine roll assessment points were displayed. The participants were required to move to the roll assessment points located at pitch/yaw configurations they reached during the coloring part of the experiment. They were also asked to try to reach the other roll assessment points but were allowed to skip them if they could not reach them.

To get familiar with the experimental procedure, each participant first conducted the experiments once with a training handle (distal type grasp). Subsequently, the experiments were conducted with the four test handles. To account for learning and fatigue effects, the order of the handles was randomized using a 4^{th} order row-complete Latin square. The experiments were conducted five times per participant (once with the training handle and four times with the test handles), and the whole experimental session took approximately 75 minutes per participant.

D. Participants

Twenty-one healthy, right-handed participants (nine females, age 23 to 35 years, mean age 27.4 years) volunteered to participate in this study. All participants had normal or corrected to normal vision and did not report any recent injury or other disorders of the right upper extremity. Six of the participants already participated in the pre-study. Other than this, the participants did not have prior experience with haptic telemanipulators. The participants were recruited from the Department of Biomedical Engineering of the University of Basel (students and researchers) and the general public. The study was conducted according to the declaration of Helsinki and the law of Switzerland and has been approved by the responsible ethics commission (EKNZ 2018-01992). Written informed consent was obtained from all participants.

One participant had to be excluded from the analysis, as during one of the roll assessments, he let go of the handle completely. The resulting uncontrolled handle motion generated invalid data for this handle. This participant had been replaced with the 21^{st} participant to guarantee that the total number of participants was a multiple of four which is required for a Latin square randomization with four conditions.

E. Data Analysis

The data collected with the training handle was not used for the data analysis. From the texture maps generated during the drawing experiment, we computed the area in the pitch/yaw configuration space that was reached by each participant. This data was then used to compute the number of participants that could reach any of the pitch/yaw configurations in the mechanical workspace of the device. This data was then used to compute the pitch/yaw workspace percentage that was reached by all participants.

The reached roll range at each of the nine roll assessment points was computed from the logged device data for each participant. The percentage of the roll workspace that was reached by all participants and each individual participant was then computed for each roll assessment point. Finally, the weighted average roll workspace percentage over all nine roll assessment points was computed for the roll workspace reached by all participants as well as for the individual participants. As for the data from the pre-study, we calculated the offsets of the pitch/yaw and roll workspace centers, $C_{\theta\psi}$ and $\overline{C}_{\varphi}$, for the different handles (see Section IV-B for details).

For the usability analysis of the different handles, only those questions of the questionnaire targeting the system usability were used (see supplemental material). These questions addressed the system usability in terms of ease of use, intuitiveness, and comfort. The scores of the individual questions were averaged over all nine relevant questions for each participant and handle, resulting in a single usability score between 0 and 100 for each participant and handle.

For the statistical analysis of the data, we used nonparametric methods, as recommended for small sample sizes [27]. An alpha level of .05 was used. To test whether the functional pitch/yaw workspace was larger with the *AdjPen* than with the *Pen*, we conducted a right-tailed Wilcoxon signed-rank test. To evaluate whether there was a change in the weighted average functional roll workspace size between the *Pen* and the *AdjPen*, we conducted a two-sided Wilcoxon signed-rank test. Similarly, we used a right-tailed Wilcoxon signed-rank test to evaluate whether the weighted average functional roll workspace was larger with the *AdjWheel* than with the *Wheel*. To evaluate

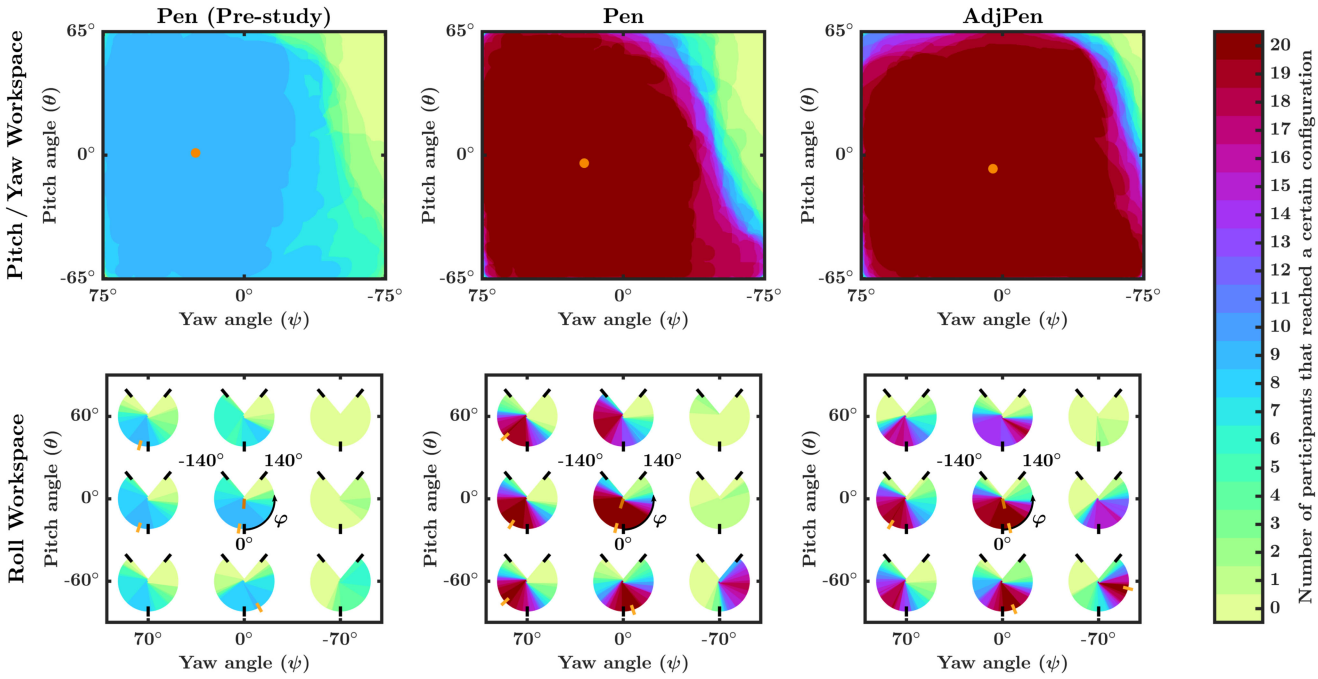

Fig. 6. Functional rotational workspace (within the virtual wall limits set to protect the device) of the participants with a fixed horizontal forearm posture for the *original writing tripod* grasp handle (*Pen*) and *pitch/yaw adjusted writing tripod* grasp handle (*AdjPen*). The workspace color indicates the number of participants that reached a certain orientational configuration. The orange circles depict the center of mass of the functional pitch/yaw workspace that was reached by all participants, $C_{\theta/\psi}$. The center of the functional roll workspace that was reached by all participants, $C_{\varphi,P_{\theta\psi}}$, is visualized by the light orange ticks for each of the nine roll assessment points $P_{\theta\psi}$. No light orange tick means that no roll configuration was reached by all participants. The dark orange tick at the center of the central circle sector depicts the weighted average center of the functional roll workspace that was reached by all participants, $\overline{C}_{\varphi}$. In the leftmost column, the data from the pre-study is visualized for comparison.

whether there was a change in the functional pitch/yaw workspace size between the *Wheel* and the *AdjWheel*, we conducted a two-sided Wilcoxon signed-rank test. To test whether the participants' center of mass of the functional pitch/yaw workspace was closer to the pitch/yaw center of mass of the device workspace with the *AdjPen* than with the *Pen*, we conducted a left-tailed Wilcoxon signed-rank test. To evaluate whether there was a change in the weighted average functional roll workspace centers between the *Pen* and the *AdjPen*, we conducted a two-sided Wilcoxon signed-rank test. Similarly, we used a left-tailed Wilcoxon signed-rank test to evaluate whether the weighted average functional roll workspace centers were closer to the mechanical roll workspace center of the device with the *AdjWheel* than with the *Wheel*. To evaluate whether there was a change in the offset of the functional pitch/yaw workspace center of mass from the device workspace center of mass between the *Wheel* and the *AdjWheel*, we conducted a two-sided Wilcoxon signed-rank test. Two-sided Wilcoxon signed-rank tests were performed to evaluate whether the usability scores of the *AdjPen* and the *AdjWheel* were different from the ones of the *Pen* and *Wheel*, respectively.

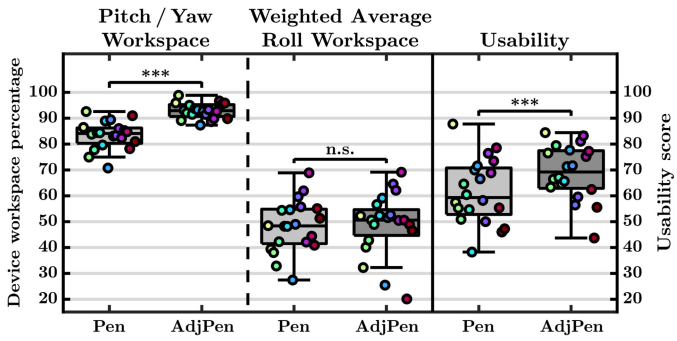

Fig. 7. Functional rotational workspace with a fixed horizontal forearm posture as percentage of the mechanical device workspace and usability scores for the *original writing tripod* grasp handle (*Pen*) and the *pitch/yaw adjusted writing tripod* grasp handle (*AdjPen*). The central mark on each box indicates the median and the bottom and top edges of the boxes designate the 25$^{\text{th}}$ (q_1) and 75$^{\text{th}}$ (q_3) percentiles, respectively. The whiskers extend to the most extreme data points not considered outliers. Data points greater than $q_3 + 1.5 \times (q_3 - q_1)$ or less than $q_1 - 1.5 \times (q_3 - q_1)$ are considered outliers. The individual data points are shown as circles on top of the box plots. Each color represents the data from one participant. Significant differences ($p < .001$) between the *Pen* and *AdjPen* are indicated with ***. A comparison without significant difference ($p \geq .05$) is indicated with n.s.

F. Results

1) Pitch/Yaw Adjustment: The functional rotational workspaces with a fixed horizontal forearm posture for the *Pen* and *AdjPen* are shown in Fig. 6. The functional pitch/yaw workspace of the individual participants with the *AdjPen* was significantly larger than with the *Pen*, ($Z = 3.901$, $p < .001$, see Fig. 7). The weighted average functional roll workspace range of the individual participants was not significantly different between the *Pen* and the *AdjPen*, ($Z = 0.933$, $p = .351$). However, the weighted average functional roll workspace range that was reached by all participants changed from $\overline{R}_{\varphi,Pen} = 48.8°$ to $\overline{R}_{\varphi,AdjPen} = 24.5°$. The offset of the functional pitch/yaw

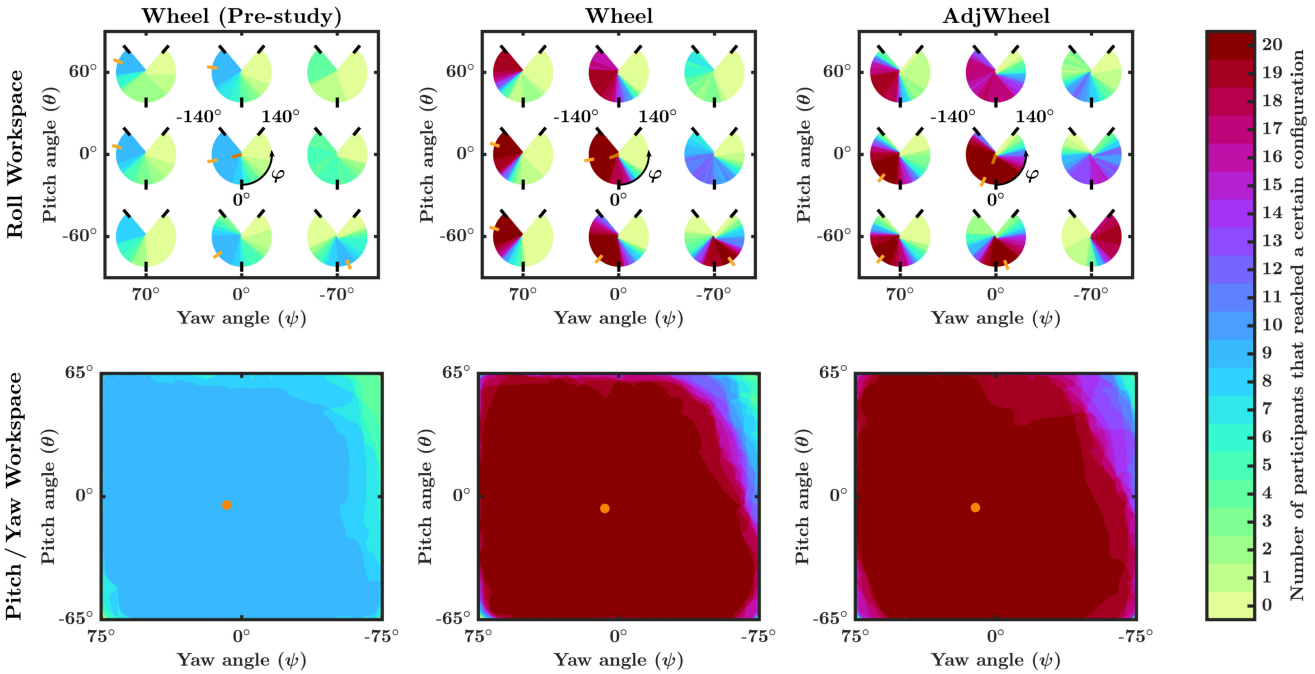

Fig. 8. Functional rotational workspace (within the virtual wall limits set to protect the device) of the participants with a fixed horizontal forearm posture for the *original precision disk* grasp handle (*Wheel*) and *roll adjusted precision disk* grasp handle (*AdjWheel*). The workspace color indicates the number of participants that reached a certain orientational configuration. The center of the functional roll workspace that was reached by all participants, $C_{\varphi,P_{\theta\psi}}$, is visualized by the light orange ticks for each of the nine roll assessment points $P_{\theta\psi}$. No light orange tick means that no roll configuration was reached by all participants. The dark orange tick at the center of the central circle sector depicts the weighted average center of the functional roll workspace that was reached by all participants, $\overline{C}_{\varphi}$. The orange circles depict the center of mass of the functional pitch/yaw workspace that was reached by all participants, $C_{\theta/\psi}$. In the leftmost column, the data from the pre-study is visualized for comparison.

workspace center reached by all participants from the center of the mechanical pitch/yaw workspace of the lambda.6 decreased: $\|C_{\theta/\psi,Pen}\| = 21.2°$, $\|C_{\theta/\psi,AdjPen}\| = 8.8°$ (see Fig. 6). Such an offset decrease was also observed at the individual participant level ($Z = -3.901$, $p < .001$). The weighted average functional roll workspace center reached by all participants changed from $\overline{C}_{\varphi,Pen} = -17.9°$ to $\overline{C}_{\varphi,AdjPen} = 12.5°$. The magnitude of the weighted average functional roll workspace center offset was not significantly different between the *Pen* and *AdjPen* at the individual participant level ($Z = -0.523$, $p = .601$). However, closer inspection of the data revealed a significant change in the location of the weighted average functional roll workspace center between the *Pen* and the *AdjPen* at the individual participant level ($Z = 3.659$, $p < .001$). A significant difference was found in the usability scores between the *Pen* and the *AdjPen* ($Z = 3.323$, $p < .001$). Closer inspection of the usability scores showed that the usability increased for the *AdjPen* compared to the *Pen* (see Fig. 7).

2) Roll Adjustment: The functional rotational workspaces with a fixed horizontal forearm posture for the *Wheel* and *AdjWheel* are shown in Fig. 8. The weighted average functional roll workspace range of the individual participants was significantly larger with the *AdjWheel* than with the *Wheel*, ($Z = 3.491$, $p < .001$, see Fig. 9). However, the weighted average functional roll workspace range that was reached by all participants changed only from $\overline{R}_{\varphi,Wheel} = 56.0°$ to $\overline{R}_{\varphi,AdjWheel} = 59.3°$. The functional pitch/yaw workspace size of the individual participants was not significantly different between the *Wheel* and the *AdjWheel*, ($Z = 0.784$, $p = .433$). The offset of the weighted average functional roll workspace center reached by all participants from 0° roll decreased: $\overline{C}_{\varphi,Wheel} = -69.1°$, $\overline{C}_{\varphi,AdjWheel} = -20.0°$ (see Fig. 8). Such an offset decrease was also observed at the individual participant level ($Z = -3.901$, $p < .001$). The offset of the functional pitch/yaw workspace center reached by all participants from the center of the mechanical pitch/yaw

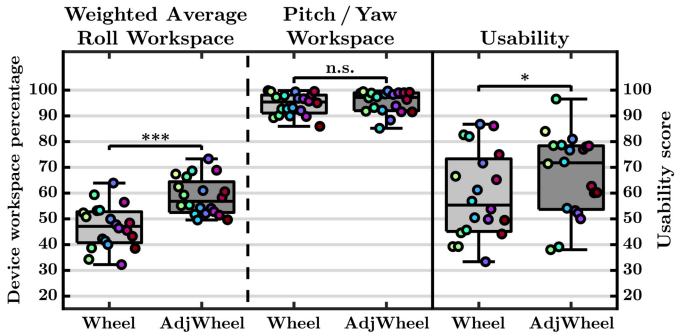

Fig. 9. Functional rotational workspace with a fixed horizontal forearm posture as percentage of the mechanical device workspace and usability scores for the *original precision disk* grasp handle (*Wheel*) and the *roll adjusted precision disk* grasp handle (*AdjWheel*). The central mark on each box indicates the median and the bottom and top edges of the boxes designate the 25th (q_1) and 75th (q_3) percentiles, respectively. The whiskers extend to the most extreme data points not considered outliers. Data points greater than $q_3 + 1.5 \times (q_3 - q_1)$ or less than $q_1 - 1.5 \times (q_3 - q_1)$ are considered outliers. The individual data points are shown as circles on top of the box plots. Each color represents the data from one participant. Significant differences between the *Wheel* and *AdjWheel* are indicated with *** ($p < .001$) and * ($p < .05$). A comparison without significant difference ($p \geq .05$) is indicated with n.s.

workspace of the lambda.6 changed slightly: $\|C_{\theta/\psi,Wheel}\| = 9.7°$, $\|C_{\theta/\psi,AdjWheel}\| = 12.3°$. The offset of the functional pitch/yaw workspace center of the *AdjWheel* was not significantly different from the one of the *Wheel* at the individual participant level ($Z = -0.635$, $p = .526$). A significant difference was found in the usability scores between the *Wheel* and the *AdjWheel* ($Z = 1.979$, $p = .048$). Closer inspection of the usability scores showed that the usability increased for the *AdjWheel* compared to the *Wheel* (see Fig. 9).

V. Discussion

Extending the work presented in [22], this study provides insights on how the grasp type and mounting orientation of a telemanipulator handle influence the telemanipulator's functional rotational workspace with a fixed horizontal forearm posture. We hypothesized that by systematically adjusting the mounting orientation of a grasp type handle with either an off-center functional pitch/yaw workspace or an off-center functional roll workspace, the functional rotational workspace with the respective grasp type handle can be increased. These hypotheses have been confirmed for two exemplary grasp type handles by the experiments described in this work. Not only was the workspace that all participants could reach more centered in the mechanical workspace of the device after the adjustment, the same was observed for the workspaces of the individual participants as well.

While previous work focused on subjective ratings of different handle concepts that also allow for the control of a seventh trigger DoF [28], we quantitatively assessed the functional rotational workspace with a fixed horizontal forearm posture for different grasp type handles and their mounting orientation using a six DoF telemanipulator. Our results suggest that both the grasp type and mounting orientation of a telemanipulator handle influence the telemanipulator's functional rotational workspace. In a first study, we observed a relation between the functional rotational workspace of different grasp type handles and the wrist configuration when holding the handles in the home configuration of the device [22]. However, the results from that study gave no insight into whether the grasp type or the home wrist configuration was the limiting factor. Thus, we conducted a second study where the functional rotational workspace of two exemplary grasp type handles was assessed with different mounting orientations. The *AdjPen* was grasped with less forearm pronation and less dorsal flexion of the wrist in the home configuration compared to the *Pen*. This led to a better reachability of negative yaw angles. On the other hand, the *AdjWheel* was grasped with less forearm pronation in the home configuration than the *Wheel*, which improved the reachability of positive roll angles. These results suggest that the home orientation of the telemanipulator handle is an important factor for the functional rotational workspace of a human-robot system.

Adjusting the pitch/yaw mounting orientation of the writing tripod grasp handle did not lead to a significant change in the functional roll workspace range at the individual participant level. However, this result has to be interpreted with care, as the weighted average functional roll workspace range reached by all participants was clearly decreased for the *AdjPen* compared to the *Pen*. In case a large functional roll workspace is needed for a given application, the pitch/yaw mounting orientation of the telemanipulator might still be of importance. We also did not find a significant change in the size of the functional pitch/yaw workspace that each individual participant could reach when the roll mounting orientation of the precision disk grasp handle was adjusted.

Compared to the pre-study, the workspaces observed in this study with the *Pen* and *Wheel* were very similar. However, the pitch/yaw workspace that could be reached by all participants with the *Pen* extended further into negative yaw. A closer inspection of the data revealed that in the pre-study, there was one participant that reached less into the negative yaw direction than all other participants. Ignoring this one outlier, the workspace assessment seems to yield robust results. We thus conclude that instead of using the workspace that all participants could reach for the adjustment of the handle orientation, it might have been more representative to use the workspace that a large majority could reach.

Surprisingly, the mounting orientation of the two investigated grasp type handles showed an influence on the usability of the handles. A possible explanation for this observation could be that the adjusted mounting orientation of the two investigated grasp type handles improved the ergonomics of the system and thus led to higher usability scores.

Our results suggest that a large functional rotational workspace with a fixed horizontal forearm posture for a telemanipulator with a symmetric yaw/pitch/roll workspace can be obtained if the handle is mounted in a telemanipulator home configuration such that there is no dorsal wrist flexion and the user's forearm is in a neutral pro-/supination configuration. This is in accordance with previous findings on ergonomics for workplaces [20] and hand tools [29]. It thus seems that designing haptic telemanipulators according to ergonomic recommendations is not only relevant to prevent musculoskeletal disorders, but also to increase the functional rotational workspace of the human-robot system as well as its usability. However, our data is not sufficient to state whether such a home configuration would maximize the functional rotational workspace for any given handle and arm posture. Especially, we only performed the workspace adjustment experiments with precision grip handles and in an ergonomic posture with a fixed horizontal forearm posture. It thus remains unknown if our findings also apply to power grip handles or considerably different arm postures.

In real teleoperation settings, the master device is mostly used to control a specific tool at the slave side. Usually, the handle is mounted such that it is grasped in the same orientation as the slave tool would be grasped. The original handles assessed in [22] were developed for a slave tool whose longitudinal axis corresponds to the x-axis of the lambda.6 haptic device (see Fig. 1). Besides, for tools having a predominant roll orientation, such as the cutting edge of a scalpel, it was assumed to point in the negative z-direction. Changing the mounting orientation of the master device handle would mean that either this handle-tool-alignment would not uphold or that the slave device would

have to be rotated with respect to the master device. According to previous findings, humans can adapt to a constant handle-tool-misalignment of up to $20-30^{\circ}$ without any negative effects on teleoperation performance [11]. Unlike applying workspace spanning techniques to orientational DoF, a handle-tool-misalignment introduced by a different mounting of the telemanipulator handle would be constant. While variable handle-tool-misalignment has been found to be confusing for the operator [7], constant handle-tool-misalignments are common also for real tools: while normal scissors have the handle aligned with the cutting edge, bandage scissors typically come with a constant handle offset of around 30°. We thus expect that choosing the telemanipulator handle orientation based on the resulting functional rotational workspace of the human-robot system is feasible for most teleoperation settings. However, whether this approach would increase the functional rotational workspace of the master device without any limitations on the intuitiveness of the system and the required mechanical workspace of the slave device for a specific teleoperation setting cannot be guaranteed.

The goal of this study was to assess if the overlap of two limited workspaces (of the haptic device and the human hand and wrist) can be increased by adjusting the mounting orientation of the device handle. Most haptic devices have a limited workspace due to a trade-off between different requirements, such as workspace, stiffness, force feedback, or cost. If the haptic device does not allow to measure the complete anatomical workspace of the human hand and wrist with a given grasp type, several iterations may be needed to maximize the overlap of the two workspaces. In our experiments the lambda.6 device was workspace-limiting. Nevertheless, we have observed satisfying overlap with a single iteration and would expect that for most workspace-limiting haptic devices a few iterations would be sufficient as well.

For this study, the participants' right forearms were strapped to the armrest. This was necessary to compare the functional rotational workspace allowed by the human hand and wrist between different handles. The strapping did not completely fix the user's forearm pose, but allowed slight motion. However, in a real surgical setting, the operator is free to move their arms while being provided with the opportunity to rest their forearms on an armrest. It is likely that without a forearm fixation, the user would simply adjust their movements and posture to the device, which would lead to a larger functional rotational workspace as reported here. However, lifting the forearms from the provided armrest has been identified as a prevalent ergonomic issue in robot-assisted surgery [19]. Ergonomic guidelines suggest that robot-assisted surgical systems should allow users to maintain their forearms resting comfortably on the provided armrest in a neutral position [20], [21]. Thus, by strapping the participants' forearms we measured the functional rotational workspace of the human-robot system that can be achieved with an ergonomic upper body and arm posture.

Based on the herein presented work, first recommendations for a systematic approach to choose and adapt a telemanipulator handle for any given application can be formulated:

1) Define the required rotational workspace for the application at hand.
2) Choose/develop a telemanipulation master device according to the workspace requirements, i.e., the master device should cover the whole required rotational workspace.
3) Select a telemanipulator handle. This may be done either based on a preferred handle shape (e.g., due to the slave tool you want to control or user experience [26]) or according to the functional rotational workspace.
4) Mount the selected handles such that in the home configuration, it is held with an ergonomic posture (neutral wrist position, neutral forearm pro-/supination, forearm supported by armrest).
5) In a user study, assess whether the functional rotational workspace of your system is sufficient for the task at hand. If necessary, adjust the functional rotational workspace of the system. This could be done by adjusting the orientation the handle is mounted to the telemanipulator as we did, or by adjusting the orientation of the whole telemanipulator as e.g. in [30]. Repeat this step if necessary.
6) Make sure your adjustments do not compromise the ergonomics of the system and that the handle-tool-alignment is still intuitive for the operator. Therefore, additional user studies might be necessary.

Previous work offers data to help decide on the telemanipulator handle (step 3) [22], [28] and an ergonomic home configuration (step 4) [20], [29]. In this work, we present one possibility for a systematic approach that could be used for step 5.

VI. Conclusion

We investigated whether the functional rotational workspace of two exemplary grasp type handles can be systematically increased by simply changing the orientation in which they are mounted to a telemanipulator. Our results indicate that such a systematic adjustment is possible and even leads to higher usability scores of the investigated handles. To achieve a high functional rotational workspace, the telemanipulator handle should be mounted such that in the telemanipulator home configuration, the user's wrist and forearm are in an ergonomic posture, i.e., that there is no dorsal wrist flexion/extension and the forearm is in a neutral pro-/supination position. However, whether such a home position is feasible for any handle and application is debatable. Therefore, we conclude that it is crucial to carefully choose a telemanipulator handle specifically for any given application.

References

[1] Intuitive Surgical, "Annual report 2018," 2018. [Online]. Available: http://www.annualreports.com/HostedData/AnnualReports/PDF/NASDAQ_ISRG_2% 018.pdf
[2] S. M. Prasad, S. M. Prasad, H. S. Maniar, C. Chu, R. B. Schuessler, and R. J. Damiano Jr, "Surgical robotics: impact of motion scaling on task performance," *J. Amer. College Surgeons*, vol. 199, no. 6, pp. 863–868, 2004.
[3] S. Park, R. D. Howe, and D. F. Torchiana, "Virtual fixtures for robotic cardiac surgery," in *Proc. Int. Conf. Med. Image Comput. Comput.-Assisted Intervention*, 2001, pp. 1419–1420.

[4] N. Enayati, E. De Momi, and G. Ferrigno, "Haptics in robot-assisted surgery: Challenges and benefits," in *IEEE Rev. Biomed. Eng.*, vol. 9, pp. 49–65, 2016.
[5] P. Schleer, P. Kaiser, S. Drobinsky, and K. Radermacher, "Augmentation of haptic feedback for teleoperated robotic surgery," *Int. J. Comput. Assisted Radiol. Surgery*, vol. 15, no. 3, pp. 515–529, 2020.
[6] E. G. Johnsen and W. R. Corliss, *Human Factors Applications in Teleoperator Design and Operation*. Hoboken, NJ, USA: Wiley-Interscience New York, 1971.
[7] A. J. Madhani, G. Niemeyer, and J. K. Salisbury, "The Black Falcon: A teleoperated surgical instrument for minimally invasive surgery," in *Proc. IEEE/RSJ Int. Conf. Intell. Robots Syst. Innovations Theory, Practice Appl. (Cat. No. 98CH36190)*, 1998, vol. 2, pp. 936–944.
[8] U. Hagn *et al.*, "DLR mirosurge: A versatile system for research in endoscopic telesurgery," *Int. J. Comput. Assisted Radiol. Surgery*, vol. 5, no. 2, pp. 183–193, 2010.
[9] F. Conti and O. Khatib, "Spanning large workspaces using small haptic devices," in *Proc. 1st Joint Eurohaptics Conf. Symp. Haptic Interfaces Virtual Environment Teleoperator Syst. World Haptics Conf.*, 2005, pp. 183–188.
[10] M. Mamdouh, A. A. Ramadan, and A. A. Abo-Ismail, "Evaluation of a proposed workspace spanning technique for small haptic device based manipulator teleoperation," in *Proc. Int. Conf. Intell. Robot. Appl.*, 2012, pp. 161–170.
[11] L. H. Kim, C. Bargar, Y. Che, and A. M. Okamura, "Effects of master-slave tool misalignment in a teleoperated surgical robot," in *Proc. IEEE Int. Conf. Robot. Autom.*, 2015, pp. 5364–5370.
[12] H. Boessenkool, J. G. Wildenbeest, C. J. Heemskerk, M. R. de Baar, M. Steinbuch, and D. A. Abbink, "A task analysis approach to quantify bottlenecks in task completion time of telemanipulated maintenance," *Fusion Eng. Des.*, vol. 129, pp. 300–308, 2018.
[13] Haption, "Virtuose^{TM} 6D Desktop," 2019. [Online]. Available: https://www.haption.com/en/products-en/virtuose-6d-desktop-en.html
[14] 3D Systems, "Advanced haptic devices for academic and commercial research and development. Technical specifications," 2016. [Online]. Available: https://www.3dsystems.com/haptics-devices/3d-systems-phantom-premium/sp% ecifications
[15] A. Tobergte *et al.*, "The sigma.7 haptic interface for MiroSurge: A new bi-manual surgical console," in *Proc. IEEE/RSJ Int. Conf. Intell. Robots Syst.*, 2011, pp. 3023–3030.
[16] K. Zareinia, Y. Maddahi, C. Ng, N. Sepehri, and G. R. Sutherland, "Performance evaluation of haptic hand-controllers in a robot-assisted surgical system," *Int. J. Med. Robot. Comput. Assisted Surgery*, vol. 11, no. 4, pp. 486–501, 2015.
[17] U. Matern, "Ergonomic deficiencies in the operating room: examples from minimally invasive surgery," *Work*, vol. 33, no. 2, pp. 165–168, 2009.
[18] S. V. Gehrmann, R. A. Kaufmann, and Z.-M. Li, "Wrist circumduction reduced by finger constraints," *J. Hand Surgery*, vol. 33, no. 8, pp. 1287–1292, 2008.
[19] R. Craven, J. Franasiak, P. Mosaly, and P. A. Gehrig, "Ergonomic deficits in robotic gynecologic oncology surgery: a need for intervention," *J. Minimally Invasive Gynecol.*, vol. 20, no. 5, pp. 648–655, 2013.
[20] L. McAtamney and E. N. Corlett, "RULA: A survey method for the investigation of work-related upper limb disorders," *Appl. Ergonomics*, vol. 24, no. 2, pp. 91–99, 1993.
[21] M. M. Lux, M. Marshall, E. Erturk, and J. V. Joseph, "Ergonomic evaluation and guidelines for use of the daVinci robot system," *J. Endourol.*, vol. 24, no. 3, pp. 371–375, 2010.
[22] E. I. Zoller, P. C. Cattin, A. Zam, and G. Rauter, "Assessment of the functional rotational workspace of different grasp type handles for the lambda.6 haptic device," in *Proc. IEEE World Haptics Conf. (WHC)*, 2019, pp. 127–132.
[23] F. Conti *et al.*, "The CHAI libraries," in *Proc. Eurohaptics*, 2003, pp. 496–500.
[24] T. Feix, J. Romero, H.-B. Schmiedmayer, A. M. Dollar, and D. Kragic, "The GRASP taxonomy of human grasp types," *IEEE Trans. Human-Mach. Syst.*, vol. 46, no. 1, pp. 66–77, Feb. 2016.
[25] E. I. Zoller, P. Salz, A. Zam, P. C. Cattin, and G. Rauter, "Development of different grasp type handles for a haptic telemanipulator," in *Proc. 9th Joint Workshop New Technol. Comput./Robot Assisted Surgery (CRAS 2019)*, 2019, pp. 22–23.
[26] L. Santos-Carreras, M. Hagen, R. Gassert, and H. Bleuler, "Survey on surgical instrument handle design: Ergonomics and acceptance," *Surgical Innovation*, vol. 19, no. 1, pp. 50–59, 2012.
[27] K. Le Boedec, "Sensitivity and specificity of normality tests and consequences on reference interval accuracy at small sample size: a computer-simulation study," *Veterinary Clinical Pathol.*, vol. 45, no. 4, pp. 648–656, 2016.
[28] T. L. Brooks and A. K. Bejczy, "Hand controllers for teleoperation. A state-of-the-art technology survey and evaluation," Jet Propulsion Laboratory, Pasadena, CA, USA, Tech. Rep. 85-11, 1985.
[29] A. Freivalds, "Ergonomics of hand tools," in *Occupational Ergonomics: Principles of Work Design*. Boca Raton, FL, USA: CRC Press, 2003, pp. 27–1–27–18.
[30] F. Gosselin, F. Ferlay, S. Bouchigny, C. Mégard, and F. Taha, "Specification and design of a new haptic interface for maxillo facial surgery," in *Proc. IEEE Int. Conf. Robot. Autom.*, 2011, pp. 737–744.

Esther I. Zoller received the B.Sc. and M.Sc. degrees in human movement sciences from ETH Zurich, Switzerland, in 2012 and 2014, respectively. In 2012, she joined the Human Performance Lab in Calgary, Canada, for an Internship and the master's thesis. She is currently working toward the Ph.D. degree in biomedical engineering from the University of Basel, Switzerland. Her research interests include haptic human-robot interaction, enhancing surgical simulation with haptics, and human perception.

Nicolas Gerig recived the B.Sc. and M.Sc. degrees in mechanical engineering with ETH Zurich, Switzerland, in 2010 and 2013, respectively. He received the Ph.D. (Dr. sc. ETH Zurich), in 2018, developing a Virtual Trainer for robot-assisted movement training. In 2012, he had joined the Florida Institute for Human and Machine Cognition (Pensacola, FL) for the master's thesis on fall prevention of a robotic leg orthosis. Since April 2018, he has been the Deputy Head of the BIROMED-Lab with the Department of Biomedical Engineering, University of Basel, Switzerland. His current research interests include the developing novel robotic surgery platforms for the Minimally Invasive Robot-Assisted Computer-guided LaserostetomE (MIRACLE) Project .

Philippe C. Cattin received the B.Sc. degree in computer science from the University of Applied Science in Brugg/Windisch, Switzerland, in 1991. He received the M.Sc. degree in computer science, in 1995, and the Ph,D, degree in robotics from ETH Zurich, Switzerland, in 2003. From 2003 to 2007, he was a Postdoctoral Fellow with the Computer Vision Laboratory with ETH Zurich. In 2007, he became an Assistant Professor with the University of Basel, Switzerland, and was promoted to Associate Professor in 2015 and Full Professor in 2019. He is the founder of the Center for medical Image Analysis and Navigation (CIAN) at the Medical Faculty of the University of Basel. He is the Founding Head and still heading the Department of Biomedical Engineering with the University of Basel. His research interests include medical image analysis, image-guided therapy, and robotics-guided laser osteotomy.

Georg Rauter received the diploma in mechanical modeling from MATMECA, Bordeaux, France, in 2006, and in mechanical engineering from TU-Graz, Austria, in 2008. In 2014, he received the Ph.D. in robotics from ETH Zurich, Switzerland. From 2014 to 2016, he was Postdoc in data analysis and rehabilitation robotics with ETH Zurich, University of Southern California, and University of Zurich. Since 2016, he has been heading the BIROMED-Lab as an Assistant Professor of Medical Robotics and Mechatronics with the Department of Biomedical Engineering, University of Basel, Switzerland. His research interests include the development of robotic and mechatronic systems with a special focus on enabling minimally invasive surgical procedures and providing new and efficient rehabilitation methods.